


## ARTICLE OPEN



# ERK1/2-dependent TSPO overactivation associates with the loss of mitophagy and mitochondrial respiration in ALS

Andrea Magri<sup>1,2</sup>, Cristiana Lucia Rita Lipari<sup>3</sup>, Pierpaolo Risiglione<sup>3</sup>, Stefania Zimbone<sup>4</sup>, Francesca Guarino<sup>2,3</sup>, Antonella Caccamo<sup>5,6,7</sup> and Angela Messina<sup>1,2,7</sup> 

© The Author(s) 2023

Mitochondrial dysfunction and the loss of mitophagy, aimed at recycling irreversibly damaged organelles, contribute to the onset of amyotrophic lateral sclerosis (ALS), a fatal neurodegenerative disease affecting spinal cord motor neurons. In this work, we showed that the reduction of mitochondrial respiration, exactly oxygen flows linked to ATP production and maximal capacity, correlates with the appearance of the most common ALS motor symptoms in a transgenic mouse model expressing SOD1 G93A mutant. This is the result of the equal inhibition in the respiration linked to complex I and II of the electron transport chain, but not their protein levels. Since the overall mitochondrial mass was unvaried, we investigated the expression of the Translocator Protein (TSPO), a small mitochondrial protein whose overexpression was recently linked to the loss of mitophagy in a model of Parkinson's disease. Here we clearly showed that levels of TSPO are significantly increased in ALS mice. Mechanistically, this increase is linked to the overactivation of ERK1/2 pathway and correlates with a decrease in the expression of the mitophagy-related marker Atg12, indicating the occurrence of impairments in the activation of mitophagy. Overall, our work sets out TSPO as a key regulator of mitochondrial homeostasis in ALS.

*Cell Death and Disease* (2023)14:122; <https://doi.org/10.1038/s41419-023-05643-0>

## INTRODUCTION

Amyotrophic lateral sclerosis (ALS) is the most common, adult-onset disorder affecting the motor system, although extra-motor manifestations are emerging [1]. ALS triggers the progressive degeneration of upper and lower motor neurons (MNs) in the brain stem and spinal cord, leading to muscle weakness, atrophy, paralysis, and death within a few years from the appearance of the first symptoms [2–4]. Although ALS is generally sporadic (sALS), in a tenth of cases it is inherited with an autosomal dominant pattern, with more than 20 genes associated with familial ALS (fALS) forms [5]. Of these, mutations in the gene encoding the antioxidant enzyme Cu/Zn Superoxide Dismutase (SOD1) account for up to 20% of familial and about 5% of sporadic cases [6, 7]. The mechanisms leading to the selective death of MNs in ALS are heterogeneous and yet not fully understood. Despite this, fALS and sALS are presumed to share the same pathological mechanisms, as they have similar clinical features [8].

Mitochondria are the energy supply stations of eukaryotic cells. Primarily, they produce ATP via oxidative phosphorylation, albeit they are essential for the maintenance of a variety of additional bioenergetic and biochemical pathways, including phospholipid biosynthesis, calcium homeostasis and cell survival [9, 10]. Among cell types, neurons are the most susceptible to mitochondrial damage: they must last the lifetime of the organism and, having axons up to one meter long, require high energy demand for

preserving their functions [11, 12]. In light of these considerations, it is not surprising that mitochondria dysfunction is a key event in the onset of neurodegenerative diseases.

Morphological and ultrastructural altered, swollen and vacuolated mitochondria were observed in many different ALS cases [13, 14]. However, most of the literature information comes from SOD1 mutant models where impaired activity of the mitochondrial electron transport (ET) chain complex I and altered organelle dynamic were observed [15–18]. Remarkably, these alterations do not depend on the loss of dismutase activity of SOD1, but rather on the gain of toxic properties which prompts SOD1 misfolding and accumulation, and its partial re-localization from cytosol to mitochondria [19–24]. Within the organelle, mutated SOD1 presumably affects protein compositions, the integrity of the mitochondrial outer membrane (MOM), ATP/ADP trafficking mediated by VDAC1 and Bcl-2 activities [25–29].

To dispose of poorly functioning mitochondria, healthy MNs have a quality control system consisting in a specific form of autophagy, called mitophagy, aimed at recycling the components of irreparably damaged mitochondria [30]. Therefore, the loss of mitophagy is rapidly emerging as a hallmark of neurodegenerative diseases. Initially, this aspect was investigated in Parkinson's disease (PD), due to the direct involvement in disease pathogenesis of the E3 ubiquitin ligase Parkin and PTEN-induced kinase 1 (PINK1), both essential for the initiation of mitophagy process [31].

<sup>1</sup>Department of Biological, Geological and Environmental Sciences, University of Catania, Catania, Italy. <sup>2</sup>we.MitoBiotech S.R.L., C.so Italia 172, Catania, Italy. <sup>3</sup>Department of Biomedical and Biotechnological Sciences, University of Catania, Catania, Italy. <sup>4</sup>Istituto di Cristallografia, Consiglio Nazionale delle Ricerche, Section of Catania, Catania, Italy. <sup>5</sup>Department of Drug and Health Sciences, University of Catania, Catania, Italy. <sup>6</sup>Department of Chemical, Biological, Pharmaceutical Sciences, University of Messina, Messina, Italy. <sup>7</sup>These authors jointly supervised this work: Antonella Caccamo, Angela Messina. <sup>✉</sup>email: mess@unicit.it  
Edited by Dr Pier Giorgio Mastroberardino

Received: 31 August 2022 Revised: 31 January 2023 Accepted: 1 February 2023

Published online: 15 February 2023

However, mutations in genes regulating mitophagy, such as those encoding optineurin and p62/sequestosome-1, have been discovered also in ALS patients and linked to the disease onset [32, 33]. In addition, alterations in this pathway were observed in models overexpressing mutated SOD1, TAR DNA-binding protein 43 (TDP-43) and FUS [34–36], all genes linked to ALS. More recently, a mitochondrial key regulator of mitophagy was identified in the Translocator Protein (TSPO) [37]. TSPO is an 18 kDa multi-drug binding protein located in the MOM found upregulated in PD patients [38]. It has been demonstrated that its expression is driven by the activation of MAPK/ERK pathway [39].

With the aim of further investigating this disease aspect, here we demonstrate that in transgenic mice expressing a G93A mutant form of human SOD1, impairments of motor abilities correlate with a significant reduction of mitochondrial respiration, precisely the oxygen consumption linked to ATP production and the maximal capacity, as the result of partial inhibition of respiration coupled to complexes I and II. This, however, is not due to a reduction in the mitochondrial mass but rather is the result of overactivation of ERK1/2 pathway, which induces TSPO overexpression via STAT3, in turn triggering a partial inhibition of mitophagy. Ultimately, here we demonstrate that TSPO is a key regulator of mitochondrial quality control also in ALS.

## RESULTS

### Congenetic SOD1 G93A mice develop typical ALS phenotype

In this work, we used the commercially available congenic strain B6.Cg-Tg(SOD1\*G93A)1Gur/J mice (here simply referred as transgenic mice). In comparison to the mostly used mixed B6SJL background carrying the same mutation, this strain shows an increased life span of about 20%, with the appearance of the overt symptoms at ~20 weeks of age [40]. At this age, as expected, we noticed high expression of SOD1 in spinal cords of transgenic mice compared to wild type (Fig. 1A).

Female and male transgenic and wild type mice were further evaluated starting at 1 month of age for body weight changes (Suppl. Fig. 1). As shown in Fig. 1B, we observed a significant reduction of about 13.5% at week 19 in the body weight of transgenic mice ( $p = 0.0043$ ,  $n = 20$ ) and 18.2% at week 20 ( $p = 0.0003$ ,  $n = 20$ ). Particularly, transgenic mice reached a maximum weight value lower than wild type ( $22.9 \pm 3.74$  vs.  $26.8 \pm 4.22$  g of control,  $p = 0.0027$ ,  $n = 20$ , Fig. 1C) and at a significant younger age ( $15.3 \pm 1.7$  vs.  $19.1 \pm 1.1$  weeks of control,  $p < 0.001$ ,  $n = 20$ , Fig. 1D). Furthermore, the disease progression correlated with a significant weight loss in transgenic mice at the week 20 ( $1.54 \pm 1$  vs.  $0.29 \pm 0.38$  gr of control,  $p < 0.001$ ,  $n = 20$ , Fig. 1E).

To evaluate motor functions, rotarod test was performed. 19 weeks old transgenic and wild type mice were trained for two days on a rod at the constant speed; then, probe trials were conducted on day 3 on an accelerating rod (1 rpm/s, up to 40 rpm). In comparison to wild type, transgenic mice showed motor impairments already during the training (Suppl. Figure 2), with a time spent on the rod of  $74.8 \pm 15.7$  s the first day and  $75.6 \pm 19.7$  s the second day (wild type performances were  $88.6 \pm 4.2$ ,  $p < 0.001$ , and  $89.7 \pm 1.3$ ,  $p = 0.0029$ ,  $n = 20$ , for day 1 and day 2, respectively). The difference between the two groups was exacerbated by the accelerating rod, where the average time spent on the rod was  $30.7 \pm 6.8$  s for transgenic and  $81.2 \pm 11.7$  s for wild type mice ( $p < 0.001$ ,  $n = 20$ , Fig. 1F).

### Impaired mitochondrial respiration is observed in transgenic mice

To evaluate mitochondrial functionality, we investigated the oxygen consumption upon different conditions by using high-resolution respirometry on fresh spinal cord tissue homogenates. Figure 2A shows a representative respirometric curve obtained

from a wild type mouse alongside the specific Substrates-Uncoupled-Inhibitors Titration (SUIT) protocol used here (see Suppl. Tab 1 for raw data). Briefly, the non-phosphorylating respiration (LEAK state) was measured after the addition of the homogenate in the cuvette, in the presence of NADH-linked substrates (pyruvate, malate and glutamate) but not adenylates [41]. Then, respiration linked to the activation of ET complexes, i.e., the oxidative phosphorylation (OXPHOS state), was assayed in the presence of saturating concentration of ADP, before and after the addition of succinate. Maximal electron input to ET chain (ET capacity) was induced with uncoupler carbonyl cyanide 3-chlorophenylhydrazone (CCCP) titration, before and after the addition of rotenone. Finally, residual respiration (ROX) was measured by the addition of antimycin.

While no differences were observed between the groups for the LEAK respiration (Fig. 2B), in comparison to wild type, transgenic mice showed a significant reduction of the OXPHOS respiration: upon stimulation of the ET chain with externally added substrates and ADP, oxygen consumption was reduced of about 15% ( $p = 0.0056$ ,  $n = 10$ , Fig. 2C); accordingly, the OXPHOS flux coupled to ADP phosphorylation, the so-called net flux, decreased in a proportional manner in transgenic mice ( $p = 0.004$ ,  $n = 10$ , Fig. 2C). Similarly, ALS pathology affected both maximal ET capacity of mitochondria and the E-Excess, a respiratory reserve used by mitochondria in stress conditions. As shown in Fig. 2D, both parameters were significantly reduced in transgenic mice (respectively,  $p = 0.0023$  and  $p = 0.0012$ ,  $n = 10$ ). Furthermore, the reduction of maximal ET capacity in transgenic mice positively correlated with the impairment in motor capacity, i.e., the time spent on the accelerating rod (Fig. 2E,  $r^2 = 0.589$ ,  $p = 0.0087$ ).

Overall, our data indicate that reduction of mitochondrial respiration occurs as the phenotypical manifestations of ALS appear.

### Complex I and II linked respiration, but not their expression or mitochondrial mass, is reduced in transgenic mice

Based on previous results, we queried whether the impairment of ET chain functioning observed in transgenic mice was due to a reduction in the activity and/or protein expression of the ET complexes that in our set-up activate the chain, as well as mitochondrial mass. The SUIT protocol in Fig. 2A, indeed, allows the measurement of respiration driven by complex I. As schematized in Fig. 3A, this was achieved upon stimulation with the NADH-linked substrates and saturating concentration of ADP, but not succinate that specifically activates complex II: in this configuration, electrons flow to complex III exclusively from complex I via the Q-junction. As reported in the histogram of Fig. 3A, a significant reduction of complex I linked oxygen flux was observed in transgenic mice compared to wild type ( $-20\%$ ,  $p = 0.0019$ ,  $n = 10$ ). This data is in accordance previous reports in cell lines and other mouse models indicating a specific impairment of complex I activity [28, 42]. To analyze if the protein levels of complex I were altered, we measured the expression of NADH ubiquinone oxidoreductase core, NDUFV1. As reported in Fig. 3B, no differences were detected between groups ( $p = 0.97$ ,  $n = 4$ ). Similar results were obtained for the protein levels of Tom20, a widely marker used to assay mitochondrial mass ( $p = 0.69$ ,  $n = 4$ ).

Next, the respiration coupled to complex II (succinate dehydrogenase, SDH) was investigated as the specific contribution to the ET capacity in the presence of succinate and after the complete inhibition of complex I with rotenone (Fig. 3C). Again, complex II linked respiration was significantly reduced in transgenic mice in comparison to wild type ( $-20\%$ ,  $p = 0.03$  vs. wild type,  $n = 10$ , Fig. 3C). Similarly to what observed previously, we did not notice any variations in the protein levels of SDHA, the main hydrophobic subunit of SDH, or VDAC1, the most abundant protein of the MOM ( $p = 0.1$  and  $p = 0.75$  respectively,  $n = 4$ , Fig. 3D). Being directly involved in the modulation of the overall

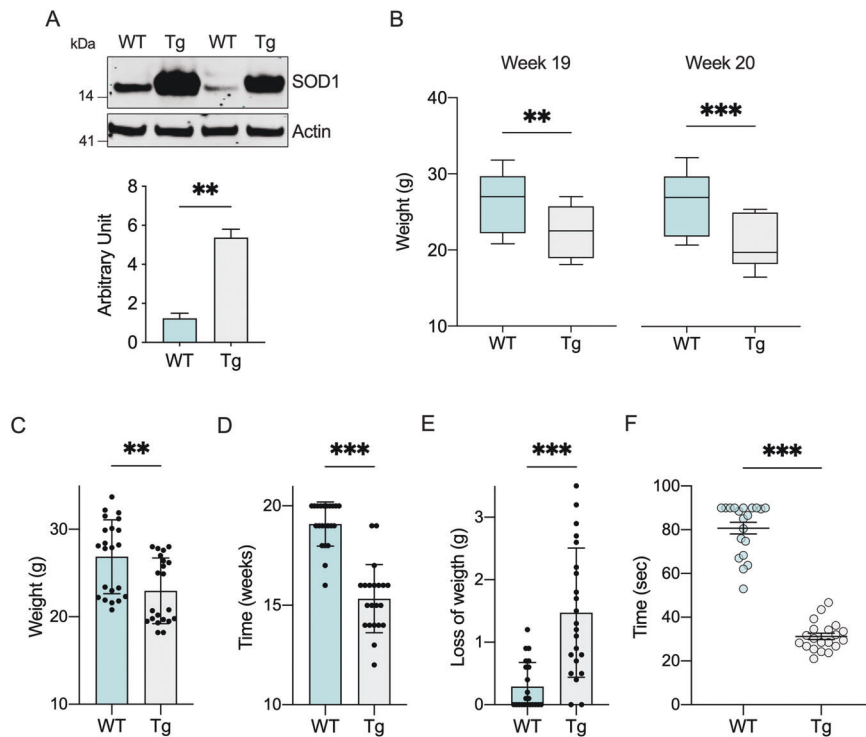


**Fig. 1 SOD1 G93A overexpression correlates with weight loss and motor impairment onset in transgenic mice.** **A** Representative Western blot of proteins extracted from spinal cord of wild type and transgenic mice and the relative quantitative analysis of SOD1. The loading control Actin was used for normalization. Data are expressed as mean  $\pm$  SEM of  $n = 2$  independent measurements. **B** Analysis of body weight related to weeks 19 and 20. Data are expressed as median  $\pm$  SEM of  $n = 20$  independent measurements. **C–E** Maximum weight reached **C**, age at the maximum weight **D**, and the weight loss at week 20 **E** relative to wild type and transgenic mice. Data are expressed as mean  $\pm$  SD of  $n = 20$  independent measurements. **F** Rotarod test performed on accelerating rod at week 20. Data are expressed as mean  $\pm$  SEM of  $n = 20$  independent measurements. All data were statistically analyzed by Student t-test, with  $**p < 0.01$  and  $***p < 0.001$ .

mitochondrial metabolic activities and acting as a physiological regulator of SDH functioning [43], we then assayed the expression levels of the NAD-dependent deacetylase sirtuin-3 (Sirt3). As reported in Fig. 3E, Sirt3 was significantly downregulated in transgenic mice compared to wild type ( $p = 0.012$ ,  $n = 4$ ).

#### Overexpression of TSPO, activated by ERK1/2, inhibits mitophagy in transgenic mice

Despite a general impairment of the ET chain activity, we did not detect any variation in the expression levels of proteins used as marker of mitochondrial mass and respiration complexes. This suggest that damaged mitochondria may accumulate in the MNs of transgenic animals. To explore this theory, we looked at TSPO, a small protein located in the MOM with a well-characterized role in the regulation of mitochondrial metabolism and a known marker of neuroinflammation and microglia activation [44]. Using a cellular model of PD, it was recently demonstrated that its overexpression correlates with a significant inhibition of mitophagy [37]. Hence, we measured the protein level of TSPO in total lysates of spinal cords by Western blot. As reported in Fig. 4A, the protein levels of TSPO were about three times higher in transgenic mice compared to wild type ( $p = 0.0004$ ,  $n = 4$ ).

To assess whether the increase in TSPO expression affected mitophagy, we measured the protein levels of the autophagy marker Atg12, which represents one of the fundamental components of the autophagosome [45]. As displayed in Fig. 4B, Atg12 levels were significantly reduced in transgenic mice: precisely, densitometric analysis revealed a reduction of about 40% in comparison to wild type ( $p = 0.016$ ,  $n = 4$ ).

It is known that TSPO expression is regulated by the MAPK/ERK pathway via STAT3 [39]. Furthermore, it has been hypothesized

that overactivation of ERK1/2 signaling cascade could play a crucial role in the development of ALS [46]. In light of these considerations, we assessed the levels of expression and phosphorylation of the proteins involved in this cascade. As showed in Fig. 5A, while the overall protein levels of ERK1 and ERK2 remained substantially unchanged, a significant increase of the phosphorylated proteins was observed exclusively in transgenic mice. Densitometric quantification indicated that levels of phosphorylated ERK1 and ERK2 were more than doubled in transgenic compared to wild type mice (Fig. 5B, C,  $p < 0.0001$ ,  $n = 4$ ). Accordingly, the downstream effector STAT3 was similarly activated: as displayed in Fig. 5A, D, the levels of STAT3 were similar between groups albeit the phosphorylated form was detected exclusively in transgenic mice ( $p = 0.0002$ ,  $n = 4$ ).

These data clearly indicate that ERK1/2-dependent TSPO overactivation correlates with the inhibition of autophagosome formation, thus with an alteration of the mitophagy process.

#### DISCUSSION

Although the large heterogeneity of the genetic and sporadic ALS, mitochondrial dysfunction characterizes all forms of the disease. Metabolic impairments arise in the early pathological stages and rapidly culminate into morphological, ultrastructural and functional abnormalities [47, 48]. Furthermore, as emerges from recent literature, ALS affected MNs show dysregulation of autophagy, which hinders the recycling of dysfunctional organelles and further aggravates the MNs function. Indeed, defects in autophagy are also responsible for the accumulation of protein aggregates and reactive oxygen species (ROS), as well as increased inflammation, all conditions that characterize ALS and other neurodegenerative diseases [49].

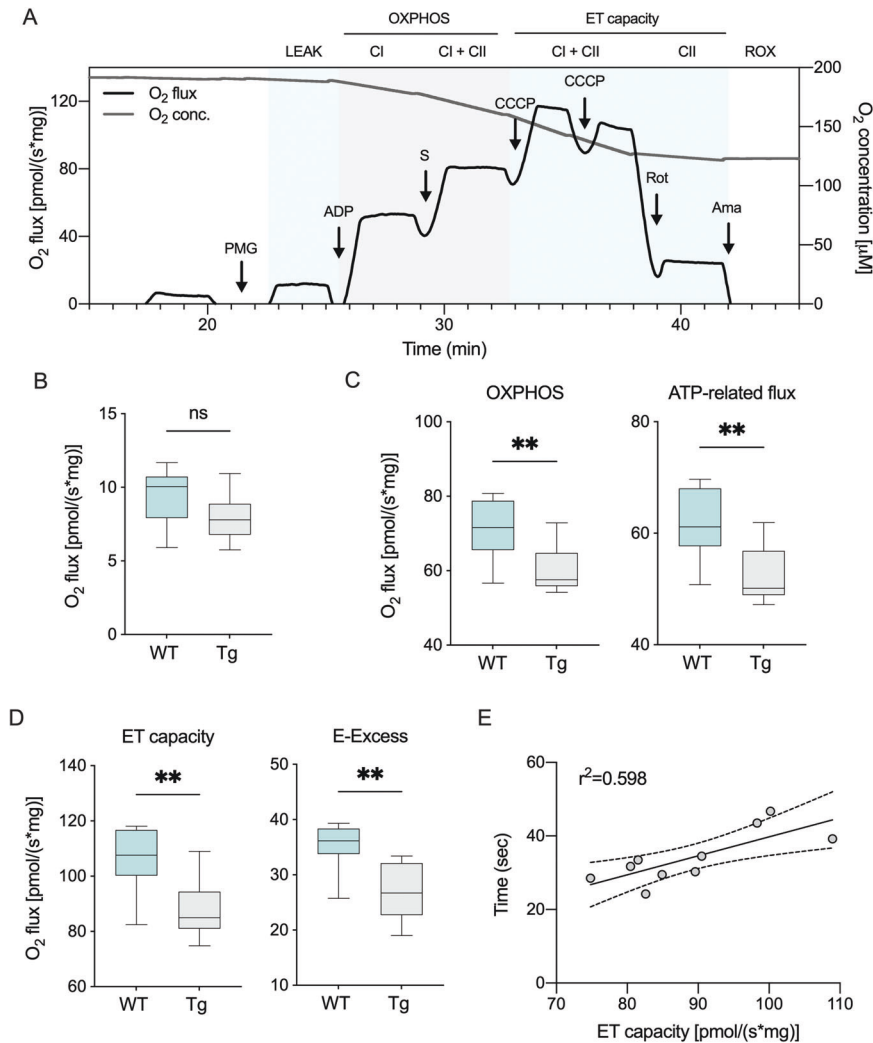


**Fig. 2 Mitochondrial respiration is impaired in transgenic mice.** **A** Representative trace of oxygen consumption achieved using homogenates from fresh spinal cords from wild type mice, and the SUIT protocol applied. Precisely, the LEAK state was measured in the presence of pyruvate, malate and glutamate (PMG) but not adenylates. The addition of ADP, followed by succinate (S), activated OXPHOS respiration sustained by complex I or complex I and II, respectively. The maximal capacity of ET chain was achieved by CCCP titration. The ET capacity sustained exclusively by complex II was measured after inhibition of complex I with rotenone (Rot). Finally, the ROX was measured after a complete inhibition of ET chain with antimycin A (Ama). **B–D** Comparative analysis of oxygen consumption in wild type and transgenic mice spinal cords' homogenates relative to LEAK **B**, OXPHOS, total and ATP-linked flow **C**, maximal ET capacity and E-Excess **D**. Data are expressed as pmol/s of oxygen per mg of tissue and as means  $\pm$  SEM of  $n = 10$  independent measurements. Data were statistically analyzed by Student t-test, with  $**p < 0.01$ ; ns not significant. **E** Correlation analysis of ET capacity with the loss of motor activities calculated as linear regression ( $r^2 = 0.598$ ,  $p = 0.0087$ ). The dotted lines represent 95% confidence intervals.

To try to understand molecular mechanisms behind this intricate puzzle, here we studied the mitochondrial dysfunction in a murine model of ALS. We found that: (i) the onset of motor dysfunctions correlates with a general decrease in oxygen consumption but not in mitochondrial mass; (ii) high level of TSPO protein expression found in the spinal cord correlates with an inhibition of mitophagy, similarly to what previously observed in PD [37].

In this work, we used the SOD1 G93A mouse model of ALS that, as expected, develops the typical ALS motor symptoms (Fig. 1). Around 20 weeks of age, spinal cords' mitochondria show a strong impairment of their functionality as demonstrated by the reduced oxygen consumption rates observed in different respiratory states. Precisely, we confirmed a significant reduction of OXPHOS-linked respiration (Fig. 2C) and the maximal capacity of the ET system (Fig. 2D). Overall, reduction of these oxygen flows has at least two important consequences. First, the ATP-related OXPHOS flux is proportionally reduced (Fig. 2C),

confirming previous data about ATP production, a key event that triggers mitochondrial dysfunction [26]. Second, the so-called E-Excess is dramatically compromised (Fig. 2D). Particularly, excess capacity is a crucial reserve to which mitochondria may rely on in cases of increase in energy demands or stress conditions [41]. In fact, the reduction of respiratory reserves are considered prodromal to mitochondrial dysfunction in many pathologies [50], as we recently observed in two different models of PD [51–53]. Thus, the concomitant reduction of ATP availability and E-Excess makes mitochondria more susceptible to further toxic insults.

Notably, reduction of respiration coupled to complex I and II, here calculated as the specific contribution of each complex in the activation of the ET chain and analyzed in real time upon the addition of specific substrates (Fig. 3A, C), is not related to variation in the protein levels of specific complexes subunits, nor to changes in mitochondrial mass, as demonstrated by Western blot in Fig. 3B, D. Certainly, inhibition of complex I in ALS is known

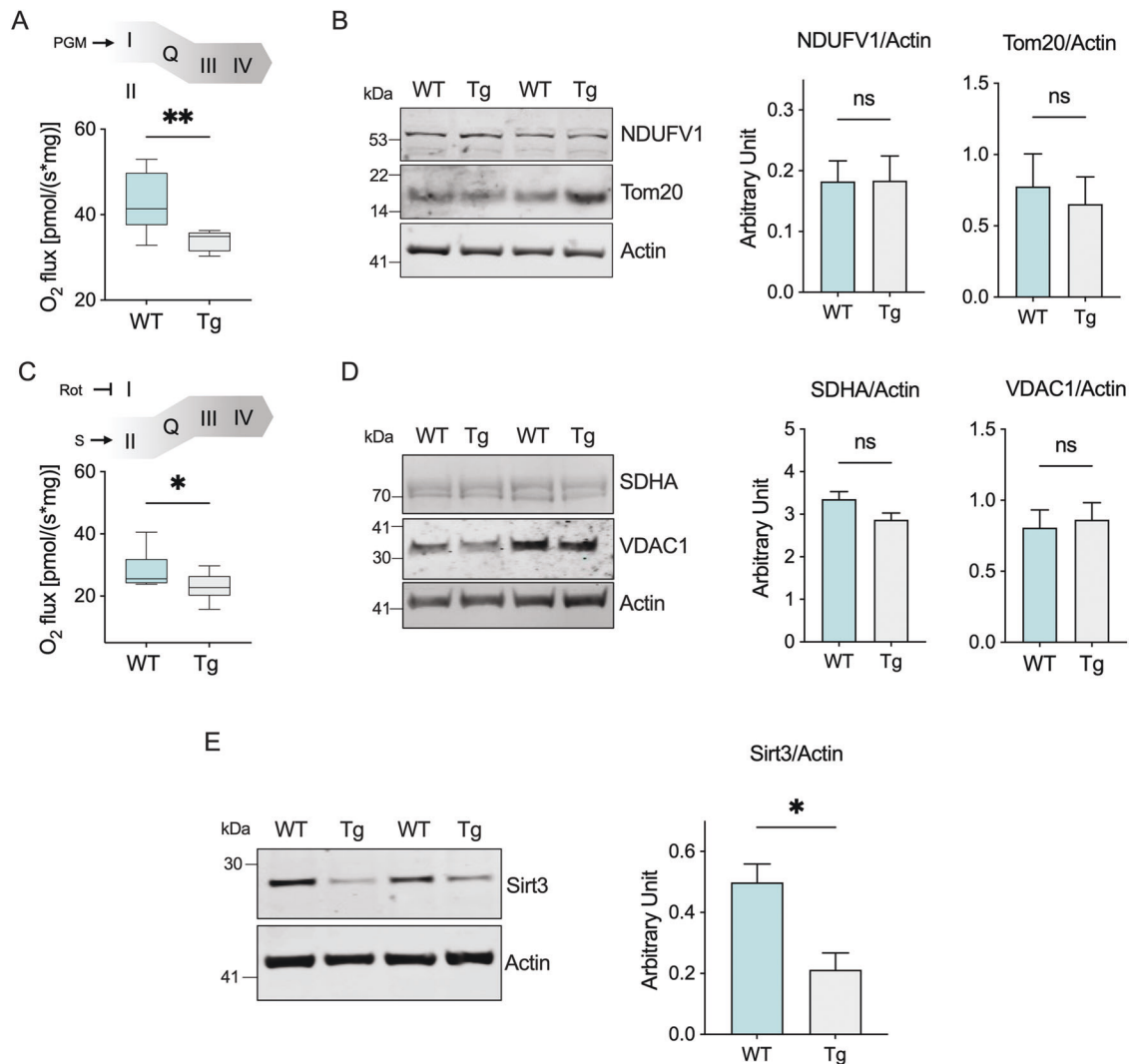


**Fig. 3 Transgenic mice show a reduced contribution in complexes I and II of the ET chain functioning but not in the mitochondrial mass.** **A** Schematic representation of the experiment rationale and comparative analysis of oxygen consumption in wild type and transgenic mice spinal cords' homogenates relative to the OXPHOS sustained by complex I. **B** Western blot of proteins extracted from spinal cords of wild type and transgenic mice and the relative quantitative analysis of NDUFV1 and Tom20. **C** Schematic representation of the experiment rationale and comparative analysis of oxygen consumption in our mice groups relative to the ET capacity sustained by complex II. **D** Western blot and the relative quantitative analysis of SDHA and VDAC1 in our samples. **E** Western blot and the relative quantitative analysis of Sirt3 in our samples. Data in **A** and **C** are expressed as pmol/s per mg of tissue and as mean  $\pm$  SEM of  $n = 10$  independent measurements. Western blot quantifications in **B**, **D**, and **E** were performed by normalizing the protein of interest to Actin, here used as loading control. Data are expressed as mean  $\pm$  SEM of  $n = 4$  independent measurement. All data were statistically analyzed by Student t-test, with  $*p < 0.05$  and  $**p < 0.01$ ; ns not significant.

since 1998 [54] and is considered a consequence of the combination of different factors, including the limited availability of NADH-linked substrates due to the deposition of SOD1 mutants on the MOM [24, 26, 55, 56]. Additionally, we found a significant reduction of Sirt3 expression in transgenic mice (Fig. 3E) that can explain the deficiency in the ET chain activity. Sirt3 is the major mitochondrial deacetylase that controls enzymes activity (including those of the ET chain), the organelle integrity and ROS homeostasis [57, 58]. In particular, SDH acts as a binding partner and substrate for the deacetylase activity of Sirt3; therefore, a reduction in Sirt3 expression may result in a decrease of SDH enzymatic activity [43]. Remarkably, downregulation of Sirt3 was recently observed in MNs derived from iPSC of both sporadic and familial ALS patients where it correlated with a reduction in mitochondrial respiration [59]. In lights of these considerations, it is conceivable that reduced protein levels of Sirt3 contribute to the impairment of ET activity.

In parallel with mitochondrial dysfunction, we noticed significant changes in TSPO expression. Physiologically, TSPO participates in a variety of mitochondrial and cellular functions, such as cholesterol import into the organelle, synthesis of heme and steroid hormones, anion transport, cell proliferation and apoptosis [60–62]. Moreover, TSPO has been widely used in the last decades as biomarker for brain imaging because it was found to increase upon injury, inflammation and the onset of neurodegenerative disorders [44, 63–66]. Interestingly, only recently the Campanella's group linked TSPO over-expression to loss of mitophagy in a cellular model of PD [37].

We observed a similar condition in our ALS model. Precisely, our results show that, in healthy spinal cords, TSPO expression is very low, consistent with data from a previous report [67], whereas in ALS its levels are about three time higher (Fig. 4A). This correlates with a significant reduction of the autophagy related protein Atg12 (Fig. 4B). Notably, Atg12 is, among Atg proteins, the one directly related to mitophagy: indeed, its overexpression exerts a

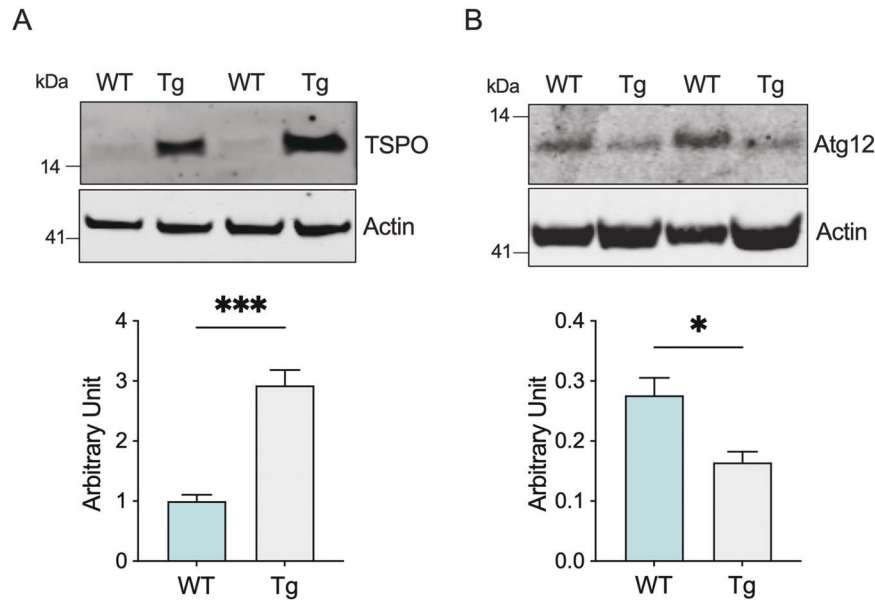


**Fig. 4 Expression of TSPO and Atg12 are inversely correlated in transgenic mice.** Western blot of proteins extracted from spinal cords of wild type and transgenic mice and the relative quantitative analysis of TSPO **A** and Atg12 **B**. Western blot quantifications were performed by normalizing the protein of interest to Actin, here used as loading control. Data in histograms are expressed as mean  $\pm$  SEM of  $n = 4$  independent measurement and statistically analyzed by Student t-test, with \* $p < 0.05$  and \*\*\* $p < 0.001$ .

protective role against mitochondrial stress insults by selectively stimulating activation of mitochondrial quality control systems [68]. Consistent with increased levels of TSPO, we noticed a significant activation of ERK1/2 signaling and STAT3 (Fig. 5), both essential for TSPO transcription [39].

ERK1/2 signaling represents one of the most important intracellular cascades for extracellular stimuli. In the nervous system, activation of ERK1/2 in response to growth factors, chemokines, cytokines and oxidative stress exerts a protective role, being involved in cell proliferation, survival and differentiation [69]. On the other side, it has been proposed that the excessive ERK phosphorylation causes neuronal abnormalities in ALS [46]. For instance, in an ALS model overexpressing TDP-43, ERK1/2 hyperactivation correlates with the accumulation of TDP-43 positive aggregates [70] and with an increase in the phosphorylation of the ERK1/2 downstream effector p90RSK [71]. Similarly, in SOD1 G93A mice an increase in ERK1/2 phosphorylation was observed in different areas of central nervous system as the pathology progresses [72]. Remarkably, ERK1/2 activation has a direct effect on mitochondrial functioning: when induced by oxidants, ERK1/2 triggers impairment of mitochondrial respiration, ATP production and substrate oxidation acting on complex I function [73]. Taken together, these data confirm the results found in this work. Thus, on one hand, ERK1/2 activation promotes TSPO overexpression via STAT3, triggering in turn mitophagy impairment; on the other hand, ERK1/2 could directly affect the ET chain function, that is already compromised by the accumulation of SOD1 mutants on the MOM and/or the reduced Sirt3 levels (see Fig. 6 for a schematization of the proposed model). Overall, these data clearly show for the first time a possible correlation between the overactivation of TSPO pathway and alterations in mitochondrial respiration and mitophagy in ALS.

In conclusion, the pathogenesis of ALS has not yet been fully elucidated, and the most accepted hypotheses attribute considerable significance to excitotoxicity, neuroinflammation, oxidative stress, and mitochondrial dysfunction. In particular, studies on mitophagy and its correlation with inflammation have become of special interest. Indeed, it is now well understood that improving mitochondrial autophagy may represent an opportunity to restore mitochondrial homeostasis, thus offering important insights into the development of potential treatments for ALS.

## MATERIALS AND METHODS

### Animals

Transgenic mice B6.Cg-Tg(SOD1\*G93A)1Gur/J (JAX ref. no. 004435), expressing high copy number of human SOD1 G93A mutant [74], and C57BL6/J wild type mice were purchased from The Jackson Laboratory (Bar Harbor, ME, USA). The colony was maintained by breeding male hemizygous carriers to wild type females in order to obtain transgenic and wild type mice. A sample size of 40 mice, 20 wild type and 20 transgenic, with an equal number of males and females, at the age-matched of 20 weeks-old was used in this study. Sample size was estimated based on information from previous studies from our and independent groups [42, 75, 76]. Mice were housed 4–5 to cage, kept on 12 h light/dark cycle and were given ad libitum access to food and water.

All experimental procedures were carried out according to the Italian Guidelines for Animal Care (D.L. 116/92 and 26/2014) and in compliance with the European Communities Council Directives (2010/63/EU). Protocols were approved by the Ethical Committee for animal experimentation at the University of Catania (OPBA, project ref. no. 334). All measures were adequately taken to minimize the number of animals used for this study.

### Genotypization

Genomic DNA was extracted from small tail biopsies by overnight digestion at 55 °C in STE lysis buffer (0.1 M Tris-HCl, pH 7.5, 5 mM EDTA, 0.2 M NaCl, 0.2% SDS) supplemented with 0.4 mg/ml of proteinase K (Sigma-Aldrich, St. Luis, MO, USA). DNA was then isolated by isopropanol-based separation and resuspended in TE buffer (10 mM Tris-HCl, pH 7.5, 1 mM EDTA, 10 mM NaCl).

Transgenic mice were identified by PCR according to manufacturer protocol. The couple of primers 5'-CAT CAG CCC TAA TCC ATC TGA-3' and 5'-CGC GAC TAA CAA TCA AAG TGA-3' was used to amplify a 236 bp product from exon 4 of the hSOD1 gene within the transgene construct. The couple of primers 5'-CTA GGC CAC AGA ATT GAA AGA TCT-3' and 5'-GTA GGT GGA TCT AGC ATC ATC C-3' was used to amplify a 324 bp product of the endogenous interleukin 2 gene, here used as DNA positive/internal control.

### Phenotypical analysis and rotarod test

To evaluate phenotypical changes, mice were weighed weekly starting at 1 month of age. Body weight loss was calculated as the difference between the maximum weight reached and the weight at the week 20. To evaluate motor functions, rotarod test was performed as in [76]. Briefly, mice were trained for 90 s (4 trials per day, for 2 consecutive days) on a rod at a constant speed of 15 rpm. Then, 4 probe trials of 90 s each were conducted

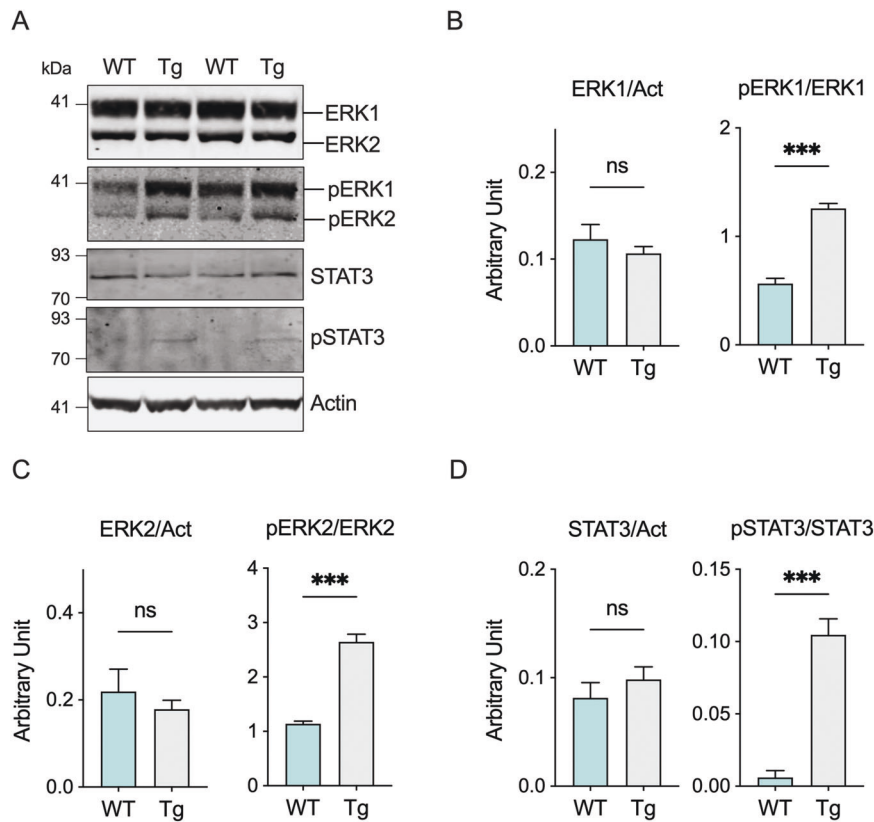


**Fig. 5 ERK1/2 signaling is activated in ALS transgenic mice.** **A** Western blot of proteins extracted from spinal cord of wild type and transgenic mice relative to total and phosphorylated ERK1/2 and STAT3. **B–D** Quantitative analysis of total and phosphorylated ERK1 **B**, ERK2 **C**, and STAT3 **D**. Western blot quantifications of total proteins were performed by normalizing the protein of interest to Actin, while quantification of phosphorylated proteins were obtained using the relative total protein for normalization. Data are expressed as mean  $\pm$  SEM of  $n = 4$  independent measurement and statistically analyzed by Student t-test, with \*\*\* $p < 0.001$ ; ns not significant.

on day 3 on an accelerating rod (1 rpm/s, up to 40 rpm). The entire set of animals was used.

#### Spinal cord extraction and tissue homogenate preparation

Animals were sacrificed by CO<sub>2</sub> asphyxiation at 20 weeks of age and spinal cords were rapidly removed. To preserve the mitochondrial functions and membranes integrity, tissue was kept in ice-cold BIOPS buffer (10 mM Ca EGTA, 20 mM imidazole, 20 mM taurine, 50 mM K-MES, 0.5 mM DTT, 6.56 mM MgCl<sub>2</sub>, 5.77 mM ATP, 15 mM phosphocreatine, Sigma-Aldrich) [77]. Alternatively, spinal cords were frozen in liquid nitrogen and stored at  $-80^{\circ}\text{C}$  for further use.

Fresh spinal cords homogenates were prepared within 1 h by using a Potter Elvehjem tissue homogenizer in mitochondrial respiration buffer Mir06 (Oroboros Instruments, Innsbruck, Austria) and immediately used for respirometric analysis.

#### High-resolution respirometry

The oxygen consumption of mitochondria was assayed in fresh spinal cord homogenates from transgenic or wild type mice by high-resolution respirometry, using the double-chamber system O2k Fluorescence Respirometer (Oroboros Instruments). Tissue homogenization protocol was tested for mitochondrial membranes integrity by cytochrome c (cyt c) assay [77, 78]. After the stimulation of respiration, 10  $\mu\text{M}$  of cyt c was added to the cuvette and any eventual run showing a significant increase in oxygen consumption, due to the cyt c entry through damaged membranes, was excluded from the analysis.

A specific SUI protocol aimed at investigating the main respiratory states was adapted from [77]. A volume of homogenate equivalent to 2 mg of the original tissue was added to the cuvette and the LEAK state was monitored in the presence of 10 mM pyruvate, 2 mM malate and 10 mM glutamate. The subsequent addition of saturating concentration of ADP (5 mM) allowed to measure OXPHOS respiration exclusively driven by complex I. Complex II was next activated by the addition of 10 mM

succinate, measuring the total OXPHOS respiration. To assay the maximal ET capacity a titration with 0.5  $\mu\text{M}$  of the uncoupler CCCP was performed. Finally, complex I was selectively inhibited with the addition of 2  $\mu\text{M}$  rotenone to achieve ET capacity linked to complex II. With the addition of 2.5  $\mu\text{M}$  antimycin, ROX was measured.

All the experiments were performed in Mir06 (Oroboros Instrument) at 37  $^{\circ}\text{C}$  under constant stirring (750 rpm). All chemicals were purchased from Sigma-Aldrich.

A set of animals of  $n = 10$  per experimental group, with an equal number of males and females, was employed for respirometric assays.

#### Respirometric data analysis

Instrumental and chemical background fluxes were calibrated as a function of the oxygen concentration using DatLab software (version 7.4.0.1, Oroboros Instruments). Rate of oxygen consumption corresponding to LEAK, OXPHOS, and ET capacity was expressed as pmol/s per milligram of tissue, and corrected for the ROX.

The ATP-related oxygen flux was calculated by normalizing the total OXPHOS flux for the LEAK respiration; the E-Excess was calculated as the difference between ET capacity and the OXPHOS respiration achieved in the presence of all substrates [51, 79]. The Pearson correlation coefficient  $r$  was calculated for transgenic mice between maximal ET capacity value and the rotarod test output (i.e., the time spent on the rod) by using Prism software (version 9, GraphPad Inc., San Diego, CA, USA).

#### Western blotting

Spinal cord were homogenized in T-PER buffer (ThermoFisher, Waltham, MA, USA) supplemented with cComplete Protease Inhibitor Cocktail (Roche, Basel, Switzerland) and Halt Phosphatase Inhibitor Cocktail (ThermoFisher) to preserve protein integrity and post-translational modifications. Total protein lysates were quantified by Pierce BCA Protein Assay Kit (ThermoFisher) and added to NuPAGE LDS sample buffer, supplemented with sample reducing agent (ThermoFisher). Approximately 30  $\mu\text{g}$  of proteins/

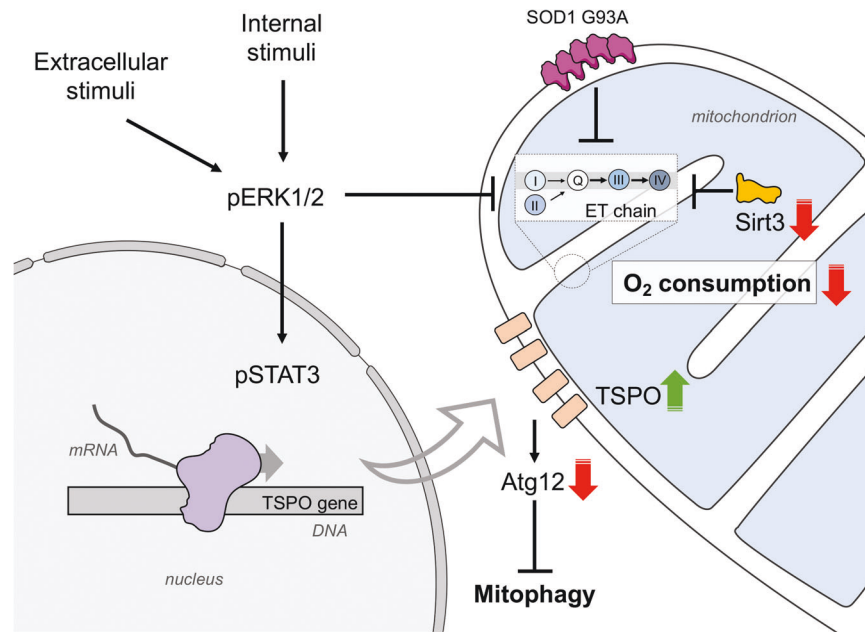


**Fig. 6 Proposed model on the role of ERK1/2 and TSPO in ALS and their involvement in mitochondrial dysfunction.** The activation of ERK1/2 signaling cascade in ALS is the sum of both external and internal stimuli and promotes TSPO overexpression via STAT3. It has been recently demonstrated that high levels of TSPO prevent the activation of mitophagy. At the same time, ERK1/2 contributes to the reduction of ET chain functioning. Notably, the enzymatic activity of ET chain is already compromised in ALS motor neurons by a sum of converging factors, including the accumulation of SOD1 G93A in the mitochondria and the lower levels of Sirt3.

sample were separated on NuPAGE Bis-Tris polyacrylamide gels (Thermo-Fisher) at 150 V for 50 min. Proteins were then transferred to nitrocellulose membranes (GE Healthcare, Boston, MA, USA) using the semi-dry system PerfectBlue Electro Blotter (Peglab, Erlangen, Germany), and the transfer was confirmed by using Ponceau S staining. Membranes were blocked in 5% BSA or not fat milk in PBS with 0.1% Tween-20. Full or portions of membranes were incubated overnight at 4 °C with primary antibodies against SOD1 (Abcam, Cambridge, UK, ref. no. ab16831, 1:1000), NDUFV1 (Immunological Sciences, ref. no. AB-83826, 1:500), Tom20 (Abcam, ref. no. ab186735, 1:500), SDHA (Abcam, ref. no. ab137040, 1:500), VDCA1 (Abcam, ref. no. ab14734, 1:1000), Sirt3 (Immunological Sciences, ref. no. AB-84353, 1:500), TSPO (Immunological Sciences, ref. no. AB-84352, 1:500), ERK1/2 (Cell Signaling, Danvers, MA, USA, ref. no. 4695, 1:2000), phospho-ERK1/2 (Cell Signaling, ref. no. 4370, 1:1000), STAT3 (Cell Signaling, ref. no. 4904, 1:500), phospho-STAT3 (Cell Signaling, ref. no. 9145, 1:500), Atg12 (Cell Signaling, ref. no. 4180, 1:1000),  $\beta$ -Actin (Cell Signaling, ref. no. 3700, 1:2000). Then, membranes were incubated with IRDye conjugated secondary antibodies (LI-COR Biosciences, Lincoln, NE, USA, 1:25,000). Signals were detected using Odyssey Imaging System (LI-COR Biosciences). Band quantification was performed by densitometric analysis using Image Studio Lite software (LI-COR Biosciences).

A set of animals of  $n = 4$  per experimental group, with an equal number of males and females, was employed for Western blot analysis.

### Statistical analysis

Data were expressed as a median or mean  $\pm$  SEM or SD and statistically analyzed by unpaired Student *t*-test using Prism software (version 9, GraphPad Inc.). The values of  $p < 0.05$ ,  $p < 0.01$ , and  $p < 0.001$  were taken as significant.

### DATA AVAILABILITY

All data generated or analyzed during this study are included in this published article and its supplementary information files.

### REFERENCES

- Phukan J, Pender NP, Hardiman O. Cognitive impairment in amyotrophic lateral sclerosis. *Lancet Neurol.* 2007;6:994–1003.
- Hardiman O, Al-Chalabi A, Chio A, Corr EM, Logroscino G, Robberecht W, et al. Amyotrophic lateral sclerosis. *Nat Rev Dis Prim.* 2017;3:17071.
- van den Bos MAJ, Geevasinga N, Higashihara M, Menon P, Vucic S. Pathophysiology and diagnosis of ALS: insights from advances in neurophysiological techniques. *Int J Mol Sci.* 2019;20:2818.
- Masrori P, van Damme P. Amyotrophic lateral sclerosis: a clinical review. *Eur J Neurol.* 2020;27:1918–29.
- Mejzini R, Flynn LL, Pitout IL, Fletcher S, Wilton SD, Akkari PA. ALS genetics, mechanisms, and therapeutics: where are we now? *Front Neurosci.* 2019;13:1310.
- Al-Chalabi A, Jones A, Troakes C, King A, Al-Sarraj S, van den Berg LH. The genetics and neuropathology of amyotrophic lateral sclerosis. *Acta Neuropathol.* 2012;124:339–52.
- Rosen DR, Siddique T, Patterson D, Figlewicz DA, Sapp P, Hentati A, et al. Mutations in Cu/Zn superoxide dismutase gene are associated with familial amyotrophic lateral sclerosis. *Nature.* 1993;362:59–62.
- Edens BM, Miller N, Ma YC. Impaired autophagy and defective mitochondrial function: converging paths on the road to motor neuron degeneration. *Front Cell Neurosci.* 2016;10:44.
- Rizzuto R, De Stefani D, Raffaello A, Mammucari C. Mitochondria as sensors and regulators of calcium signalling. *Nat Rev Mol Cell Biol.* 2012;13:566–78.
- Herst PM, Rowe MR, Carson GM, Berridge MV. Functional mitochondria in health and disease. *Front Endocrinol.* 2017;8:296.
- Payne BAI, Chinnery PF. Mitochondrial dysfunction in aging: Much progress but many unresolved questions. *Biochim Biophys Acta Bioenerg.* 2015;1847:1347–53.
- Zala D, Hincckelmann MV, Yu H, Lyra Da Cunha MM, Liot G, Cordelières FP, et al. Vesicular glycolysis provides on-board energy for fast axonal transport. *Cell.* 2013;152:479–91.
- Sasaki S, Iwata M. Mitochondrial alterations in the spinal cord of patients with sporadic amyotrophic lateral sclerosis. *Neuropathol Exp Neurol.* 2007;66:10–16.
- Smith EF, Shaw PJ, de Vos KJ. The role of mitochondria in amyotrophic lateral sclerosis. *Neurosci Lett.* 2019;710:132933.
- Coussee E, de Smet P, Bogaert E, Elens I, van Damme P, Willems P, et al. G37R SOD1 mutant alters mitochondrial complex I activity, Ca<sup>2+</sup> uptake and ATP production. *Cell Calcium.* 2011;49:217–25.
- Mattiazzi M, D'Aurelio M, Gajewski CD, Martushova K, Kiaei M, Flint Beal M, et al. Mutated human SOD1 causes dysfunction of oxidative phosphorylation in mitochondria of transgenic mice. *J Biol Chem.* 2002;277:29626–33.
- Magrané J, Sahawneh MA, Przedborski S, Estévez ÁG, Manfredi G. Mitochondrial dynamics and bioenergetic dysfunction is associated with synaptic alterations in mutant SOD1 motor neurons. *J Neurosci.* 2012;32:229–42.
- Magrané J, Hervias I, Henning MS, Damiano M, Kawamata H, Manfredi G. Mutant SOD1 in neuronal mitochondria causes toxicity and mitochondrial dynamics abnormalities. *Hum Mol Gen.* 2009;18:4552–64.



19. Bruijn LI, Houseweart MK, Kato S, Anderson KL, Anderson SD, Ohama E, et al. Aggregation and motor neuron toxicity of an ALS-linked SOD1 mutant independent from wild-type SOD1. *Science*. 1998;281:1851–4.
20. Tiwari A, Xu Z, Hayward LJ. Aberrantly increased hydrophobicity shared by mutants of Cu,Zn-superoxide dismutase in familial amyotrophic lateral sclerosis. *J Biol Chem*. 2005;280:29771–9.
21. Huai J, Zhang Z. Structural properties and interaction partners of familial ALS-associated SOD1 mutants. *Front Neurol*. 2019;10:527.
22. Shaw BF, Valentine JS. How do ALS-associated mutations in superoxide dismutase 1 promote aggregation of the protein? *Trends Biochem Sci*. 2007;32:78–85.
23. Sau D, de Biasi S, Vitellaro-Zuccarello L, Riso P, Guarnieri S, Porrini M, et al. Mutation of SOD1 in ALS: a gain of a loss of function. *Hum Mol Genet*. 2016;16:1604–18.
24. Vande Velde C, Miller TM, Cashman NR, Cleveland DW. Selective association of misfolded ALS-linked mutant SOD1 with the cytoplasmic face of mitochondria. *Proc Natl Acad Sci USA*. 2008;105:4022–7.
25. Li Q, Velde CV, Israelson A, Xie J, Bailey AO, Dong MQ, et al. ALS-linked mutant superoxide dismutase 1 (SOD1) alters mitochondrial protein composition and decreases protein import. *Proc Natl Acad Sci USA*. 2010;107:21146–51.
26. Israelson A, Arbel N, da Cruz S, Ilieva H, Yamanaka K, Shoshan-Barmatz V, et al. Misfolded mutant SOD1 directly inhibits VDAC1 conductance in a mouse model of inherited ALS. *Neuron*. 2010;67:575–87.
27. Magri A, Belfiore R, Reina S, Tomasello MF, di Rosa MC, Guarino F, et al. Hexokinase I N-terminal based peptide prevents the VDAC1-SOD1 G93A interaction and re-establishes ALS cell viability. *Sci Rep*. 2016;6:34802.
28. Magri A, Risiglione P, Caccamo A, Formicola B, Tomasello MF, Arrigoni C, et al. Small Hexokinase 1 peptide against toxic SOD1 G93A mitochondrial accumulation in ALS rescues the ATP-related respiration. *Biomedicines*. 2021;9:948.
29. Pasinelli P, Belford ME, Lennon N, Bacskai BJ, Hyman BT, Trotti D, et al. Amyotrophic lateral sclerosis-associated SOD1 mutant proteins bind and aggregate with Bcl-2 in spinal cord mitochondria. *Neuron*. 2004;43:19–30.
30. Hamacher-Brady A, Brady NR. Mitophagy programs: mechanisms and physiological implications of mitochondrial targeting by autophagy. *Cell Mol Life Sci*. 2016;73:775–95.
31. Ge P, Dawson VL, Dawson TM. PINK1 and Parkin mitochondrial quality control: a source of regional vulnerability in Parkinson's disease. *Mol Neurodegener*. 2020;15:20.
32. Maruyama H, Morino H, Ito H, Izumi Y, Kato H, Watanabe Y, et al. Mutations of optineurin in amyotrophic lateral sclerosis. *Nature*. 2010;465:233–6.
33. Fecto F, Yan J, Vemula SP, Liu E, Yang Y, Chen W, et al. SQSTM1 mutations in familial and sporadic amyotrophic lateral sclerosis. *Arch Neurol*. 2011;68:1440–6.
34. Xie Y, Zhou B, Lin MY, Wang S, Foust KD, Sheng ZH. Endolysosomal deficits augment mitochondria pathology in spinal motor neurons of asymptomatic fALS mice. *Neuron*. 2015;87:355–70.
35. Hong K, Li Y, Duan W, Guo Y, Jiang H, Li W, et al. Full-length TDP-43 and its C-terminal fragments activate mitophagy in NSC34 cell line. *Neurosci Lett*. 2012;530:144–9.
36. Cha SJ, Choi HJ, Kim HJ, Choi EJ, Song KH, Im DS, et al. Parkin expression reverses mitochondrial dysfunction in fused in sarcoma-induced amyotrophic lateral sclerosis. *Insect Mol Biol*. 2020;29:56–65.
37. Frison M, Faccenda D, Abeti R, Rigon M, Strobbe D, England-Rendon BS, et al. The translocator protein (TSPO) is prodromal to mitophagy loss in neurotoxicity. *Mol Psychiatry*. 2021;26:2721–39.
38. Gerhard A. TSPO imaging in parkinsonian disorders. *Clin Transl Imaging*. 2016;4:183–90.
39. Batarseh A, Li J, Papadopoulos V. Protein kinase C $\epsilon$  regulation of translocator protein (18 kDa) Tspo gene expression is mediated through a MAPK pathway targeting STAT3 and c-Jun transcription factors. *Biochemistry*. 2010;49:4766–78.
40. Wooley CM, Sher RB, Kale A, Frankel WN, Cox GA, Seburn KL. Gait analysis detects early changes in transgenic SOD1(G93A) mice. *Muscle Nerve*. 2005;32:43–50.
41. Gnaiger E. Capacity of oxidative phosphorylation in human skeletal muscle. New perspectives of mitochondrial physiology. *Int J Biochem Cell Biol*. 2009;41:1837–45.
42. Cacabelos D, Ramírez-Núñez O, Granada-Serrano AB, Torres P, Ayala V, Moiseeva V, et al. Early and gender-specific differences in spinal cord mitochondrial function and oxidative stress markers in a mouse model of ALS. *Acta Neuropathol Commun*. 2016;4:3.
43. Finley LWS, Haas W, Desquiret-Dumas V, Wallace DC, Procaccio V, Gygi SP, et al. Succinate dehydrogenase is a direct target of Sirtuin 3 deacetylase activity. *PLoS ONE*. 2011;6:e23295.
44. Lavisé S, Goutal S, Wimberley C, Tonietto M, Bottlaender M, Gervais P, et al. Increased microglial activation in patients with Parkinson disease using [18F]-DPA714 TSPO PET imaging. *Parkinsonism Relat Disord*. 2021;82:29–36.
45. Hanada T, Noda NN, Satomi Y, Ichimura Y, Fujioka Y, Takao T, et al. The Atg12-Atg5 conjugate has a novel E3-like activity for protein lipidation in autophagy. *J Biol Chem*. 2007;282:37298–302.
46. Sahu R, Upadhyay S, Mehan S. Inhibition of extracellular regulated kinase (ERK)-1/2 signaling pathway in the prevention of ALS: target inhibitors and influences on neurological dysfunctions. *Eur J Cell Biol*. 2021;100:151179.
47. Gautam M, Gunay A, Chandel NS, Ozdinler PH. Mitochondrial dysregulation occurs early in ALS motor cortex with TDP-43 pathology and suggests maintaining NAD<sup>+</sup> balance as a therapeutic strategy. *Sci Rep*. 2022;12:4287.
48. Myoung JC, Suh YL. Ultrastructural changes of mitochondria in the skeletal muscle of patients with amyotrophic lateral sclerosis. *Ultrastruct Pathol*. 2002;26:3–7.
49. Choi AMK, Ryter SW, Levine B. Autophagy in human health and disease. *N Engl J Med*. 2013;368:651–62.
50. Marchetti P, Fovez Q, Germain N, Khamari R, Kluz J. Mitochondrial spare respiratory capacity: mechanisms, regulation, and significance in non-transformed and cancer cells. *FASEB J*. 2020;34:13106–24.
51. Risiglione P, Cubisino SAM, Lipari CLR, De Pinto V, Messina A, Magri A.  $\alpha$ -synuclein A53T promotes mitochondrial proton gradient dissipation and depletion of the organelle respiratory reserve in a neuroblastoma cell line. *Life*. 2022;12:894.
52. Risiglione P, Leggio L, Cubisino SAM, Reina S, Paternò G, Marchetti B, et al. High-resolution respirometry reveals MPP<sup>+</sup> mitochondrial toxicity mechanism in a cellular model of Parkinson's disease. *Int J Mol Sci*. 2020;21:7809.
53. Leggio L, L'episcopo F, Magri A, Ulloa-Navas J, Paternò G, Vivarelli S, et al. Small extracellular vesicles secreted by nigrostriatal astrocytes rescue cell death and preserve mitochondrial function in Parkinson's disease. *Adv Healthc Mater*. 2022;11:2201203.
54. Browne SE, Bowling AC, Baik MJ, Gurney M, Brown RH, Beal MF. Metabolic dysfunction in familial, but not sporadic, amyotrophic lateral sclerosis. *J Neurochem*. 1998;71:281–7.
55. Magri A, Messina A. Interactions of VDAC with proteins involved in neurodegenerative aggregation: an opportunity for advancement on therapeutic molecules. *Curr Med Chem*. 2017;24:4470–87.
56. Liu J, Lillo C, Jonsson PA, Vande Velde C, Ward CM, Miller TM, et al. Toxicity of familial ALS-linked SOD1 mutants from selective recruitment to spinal mitochondria. *Neuron*. 2004;43:5–17.
57. Ansari A, Rahman MS, Saha SK, Saikot FK, Deep A, Kim KH. Function of the SIRT3 mitochondrial deacetylase in cellular physiology, cancer, and neurodegenerative disease. *Aging Cell*. 2017;16:4–16.
58. Lombard DB, Alt FW, Cheng H-L, Bunkenborg J, Streeper RS, Mostoslavsky R, et al. Mammalian Sir2 homolog SIRT3 regulates global mitochondrial lysine acetylation. *Mol Cell Biol*. 2007;27:8807–14.
59. Hor JH, Santosa MM, Lim VJW, Ho BX, Taylor A, Khong ZJ, et al. ALS motor neurons exhibit hallmark metabolic defects that are rescued by SIRT3 activation. *Cell Death Differ*. 2021;28:1379–97.
60. Papadopoulos V, Baraldi M, Guilarte TR, Knudsen TB, Lacapère JJ, Lindemann P, et al. Translocator protein (18 kDa): new nomenclature for the peripheral-type benzodiazepine receptor based on its structure and molecular function. *Trends Pharm Sci*. 2006;27:402–9.
61. Veenman L, Papadopoulos V, Gavish M. Channel-like functions of the 18-kDa Translocator Protein (TSPO): regulation of apoptosis and steroidogenesis as part of the host-defense response. *Curr Pharm Des*. 2007;13:2385–405.
62. Caballero B, Veenman L, Gavish M. Role of mitochondrial Translocator Protein (18 kDa) on mitochondrial-related cell death processes. *Recent Pat Endocr Metab Immune Drug Disco*. 2013;7:86–101.
63. Edison P, Archer HA, Gerhard A, Hinz R, Pavese N, Turkheimer FE, et al. Microglia, amyloid, and cognition in Alzheimer's disease: an [11C](R)PK11195-PET and [11C] PIB-PET study. *Neurobiol Dis*. 2008;32:412–9.
64. Pannell M, Economopoulos V, Wilson TC, Kersemans V, Isenegger PG, Larkin JR, et al. Imaging of translocator protein upregulation is selective for pro-inflammatory polarized astrocytes and microglia. *Glia*. 2020;68:280–97.
65. Turner MR, Cagnin A, Turkheimer FE, Miller CCJ, Shaw CE, Brooks DJ, et al. Evidence of widespread cerebral microglial activation in amyotrophic lateral sclerosis: An [11C](R)-PK11195 positron emission tomography study. *Neurobiol Dis*. 2004;15:601–9.
66. James ML, Belichenko NP, Nguyen TV, Andrews LE, Ding Z, Liu H, et al. PET imaging of translocator protein (18 kDa) in a mouse model of Alzheimer's disease using N-(2,5-dimethoxybenzyl)-2-18F-fluoro-N-(2-phenoxyphenyl)acetamide. *J Nucl Med*. 2015;56:311–6.
67. Daugherty DJ, Selvaraj V, Chechneva OV, Liu XB, Pleasure DE, Deng WA. TSPO ligand is protective in a mouse model of multiple sclerosis. *EMBO Mol Med*. 2013;5:891–903.
68. Mai S, Muster B, Bereiter-Hahn J, Jendrach M. Autophagy proteins LC3B, ATG5 and ATG12 participate in quality control after mitochondrial damage and influence life span. *Autophagy*. 2012;8:47–62.
69. Lavoie H, Gagnon J, Therrien M. ERK signalling: a master regulator of cell behaviour, life and fate. *Nat Rev Mol Cell Biol*. 2020;21:607–32.

70. Ayala V, Granado-Serrano AB, Cacabelos D, Naudí A, Ilieva EV, Boada J, et al. Cell stress induces TDP-43 pathological changes associated with ERK1/2 dysfunction: Implications in ALS. *Acta Neuropathol.* 2011;122:259–70.
71. Mitra J, Hegde PM, Hegde ML. Loss of endosomal recycling factor RAB11 coupled with complex regulation of MAPK/ERK/AKT signaling in postmortem spinal cord specimens of sporadic amyotrophic lateral sclerosis patients. *Mol Brain.* 2019;12:55.
72. Yoon HC, Kyeong MJ, Heon CL, Mi HC, Kim D, Won BL, et al. Immunohistochemical study on the distribution of phosphorylated extracellular signal-regulated kinase (ERK) in the central nervous system of SOD1G93A transgenic mice. *Brain Res.* 2005;1050:203–9.
73. Nowak G, Clifton GL, Godwin ML, Bakajsova D. Activation of ERK1/2 pathway mediates oxidant-induced decreases in mitochondrial function in renal cells. *Am J Physiol Ren Physiol.* 2006;291:F840–F855.
74. Gurney ME, Pu H, Chiu AY, Dal Canto MC, Polchow CY, Alexander DD, et al. Motor neuron degeneration in mice that express a human Cu,Zn superoxide dismutase mutation. *Science.* 1994;264:1772–5.
75. Caccamo A, Magri A, Oddo S. Age-dependent changes in TDP-43 levels in a mouse model of Alzheimer disease are linked to A $\beta$  oligomers accumulation. *Mol Neurodegener.* 2010;5:51.
76. Caccamo A, Magri A, Medina DX, Wisely EV, López-Aranda MF, Silva AJ, et al. mTOR regulates tau phosphorylation and degradation: implications for Alzheimer's disease and other tauopathies. *Aging Cell.* 2013;12:370–80.
77. Cantó C, Garcia-Roves PM. High-resolution respirometry for mitochondrial characterization of ex vivo mouse tissues. *Curr Protoc Mouse Biol.* 2015;5:135–53.
78. Gnaiger E, Kuznetsov AV. Mitochondrial respiration at low levels of oxygen and cytochrome c. *Biochem Soc Trans.* 2002;30:252–8.
79. Pesta D, Gnaiger E. High-resolution respirometry: OXPHOS protocols for human cells and permeabilized fibers from small biopsies of human muscle. *Methods Mol Biol.* 2012;810:25–58.

## ACKNOWLEDGEMENTS

We are grateful to Salvatore Oddo (University of Messina) and Vito De Pinto (University of Catania) for their valuable support and for the critical discussion of the data. Authors also acknowledge Fondi di Ateneo 2020–2022, Università di Catania, linea Open Access, and Attraction and International Mobility (AIM) program, Linea 1, Salute.

## AUTHOR CONTRIBUTIONS

A Magri performed behavior and respirometric experiments, analyzed and interpreted the data, draw pictures, wrote the original draft and reviewed the manuscript. CLRL participated in behavior experiments and performed Western blot. PR participated in respirometric and Western blot experiments, and analyzed the data. SZ performed mouse breeding, genotypization and samples collection, and participated in behavior experiments. FG analyzed the data and reviewed the manuscript. AC designed the study, supervised all animal experiments, analyzed and interpreted the data, contributed to original draft preparation and reviewed the

manuscript. A Messina conceptualized, designed and supervised the study, analyzed and interpreted the data, contributed to original draft preparation, reviewed and finalized the final version of the manuscript.

## FUNDING

This research was funded by Proof of Concept (grant no. PEPPLA POC 01\_00054) and PIACERI (grant no. ARVEST) to A. Messina, AIM Linea 1–Salute (AIM1833071) to A. Magri, AIM Linea 1–Salute (AIM1872330) to A. Caccamo.

## COMPETING INTERESTS

The authors declare no competing interests.

## ETHICS APPROVAL AND CONSENT TO PARTICIPATE

Not applicable

## ADDITIONAL INFORMATION

**Supplementary information** The online version contains supplementary material available at <https://doi.org/10.1038/s41419-023-05643-0>.

**Correspondence** and requests for materials should be addressed to Angela Messina.

**Reprints and permission information** is available at <http://www.nature.com/reprints>

**Publisher's note** Springer Nature remains neutral with regard to jurisdictional claims in published maps and institutional affiliations.



**Open Access** This article is licensed under a Creative Commons Attribution 4.0 International License, which permits use, sharing, adaptation, distribution and reproduction in any medium or format, as long as you give appropriate credit to the original author(s) and the source, provide a link to the Creative Commons license, and indicate if changes were made. The images or other third party material in this article are included in the article's Creative Commons license, unless indicated otherwise in a credit line to the material. If material is not included in the article's Creative Commons license and your intended use is not permitted by statutory regulation or exceeds the permitted use, you will need to obtain permission directly from the copyright holder. To view a copy of this license, visit <http://creativecommons.org/licenses/by/4.0/>.

© The Author(s) 2023